Revealing radiationless sources with multi-harmonic mantle cloaking

Revealing Radiationless Sources with Multi-harmonic Mantle Cloaking

Giuseppe Labate[1*], Andrea Massaccesi[2] and Santi C. Pavone[3]

[1]Wave Up S.r.l. - Innovation in Electromagnetics, via Roma 77, 53100 Siena, Italy.
[2]Department of Electronics and Telecomunications, Politecnico di Torino, Corso Duca degli Abruzzi 24, 10129 Torino, Italy.
[3]Department of Electrical, Electronics and Computer Engineering (DIEEI), University of Catania, viale Andrea Doria 6, 95125 Catania, Italy.

E-mail: `giuseppe.labate@wave-up.it`
February 2020

Abstract. A general formula for the scattering suppression of simultaneous cylindrical harmonic waves is reported for a bare dielectric cylinder. A proper surface impedance condition is imposed at the boundary between dielectric and background regions, revealing a parity-time condition for the internal electromagnetic field in order to be nonradiating. Depending on the maximum number M_{max} of cylindrical harmonic waves to suppress along the azimuthal variable ϕ, such surface impedance function profile reveals several higherorder nonradiating modes. The determination of M_{max} is consistent with the degrees of freedom of the scattered fields. Moreover, the multi-harmonic mantle cloaking technique automatically generates radiationless sources suitable for the implementation with metal-dielectric metasurfaces or all-dielectric metamolecules.

Keywords: cloaking, electromagnetic scattering, impedance metasurfaces, radiationless sources

Submitted to: *Journal of Optics*

1. Introduction

A radiationless source is characterized by the remarkable property of possessing localized energy, due to the fact that the electromagnetic field vanishes at all points outside the source region. In 1973, five generalized theorems have been derived by Devaney and Wolf [1] in order to find radiationless current distributions as solutions of Maxwell's equations with nontrivial internal electric field configurations. Several research efforts followed to derive other peculiar configurations of radiationless sources in terms of internal null-electric (or magnetic) field [2], internal singular values of the electromagnetics fields forming embedded (optical bound) eigenstates [3] or internal interfering electromagnetic multipoles creating anapole modes [4, 5, 6, 7]. Rather than considering specific conditions on internal total fields, the design of invisibility cloaks [8, 9, 10, 11] has been performed by considering the external electromagnetic fields and imposing to zero the ideal scattered (electric or magnetic) energy associated to undesired radiation: this unique condition automatically guarantees the generation of internal nontrivial current distributions. The cloaking behaviour of volumetric dielectric coatings based on Transformation Optics [12] has been analyzed in terms of nonradiating sources in [13], but the recent technique based on a thin surface impedance coating, named as mantle cloaking [14, 15, 16], has not completely been explored in terms of radiationless sources. Early investigations started from theorem III of Devaney-Wolf where, from the zero external scattered field specification, the related condition on internal currents and fields has been automatically obtained in the subwavelength limit [17]. Moreover, a recent generalization for elementary anapole modes has been derived from Devaney-Wolf theorem V [18].

In order to extend the validity of the closed-form surface impedance cloak design beyond the quasi-static frequency regime, an additional generalization has been proposed, namely the suppression of the first dominant external scattering harmonic wave in the case of a bare dielectric particle [19]. A further extension has been proposed for conductive objects [20], where the thin impedance cloak has to be detached at a distance $r = b$ from the boundary of the object at $r = a$ $(b > a)$.

The motivation of the work presented here is to further generalize for dielectric objects the derivation of a thin impedance layer, directly attached to the object boundary to suppress all (and not a single one) harmonic waves scattered by the bare particle. In addition, all the investigations are guided towards both external and internal electromagnetic fields, by achieving both multi-harmonic suppression in the exterior domain (multi-harmonic mantle cloaking) and, at the same time, the generation of higher-order modes (radiationless sources) in the internal domain, in which scattered energy has been trapped inside. To this purpose, a mantle cloaking technique is proposed for a dielectric cylinder, in order to cancel more than one harmonic wave simultaneously by means of a surface impedance conveniently tailored, as shown in Fig. 1. The peculiar properties of such a thin surface impedance layer are obtained in terms of the dielectric permittivity, geometrical radius and number of harmonic waves to suppress. A parity-time condition for the surface impedance function is demonstrated to hold, resulting in an oscillating azimuthal complex impedance: this is consistent with the case of a balanced loss/gain metasurface as derived for conductive objects [16]. However, conversely to a conductive object, the case of a single bare dielectric particle permits non-zero internal electromagnetic fields while ensuring the suppression of external scattered waves: with the

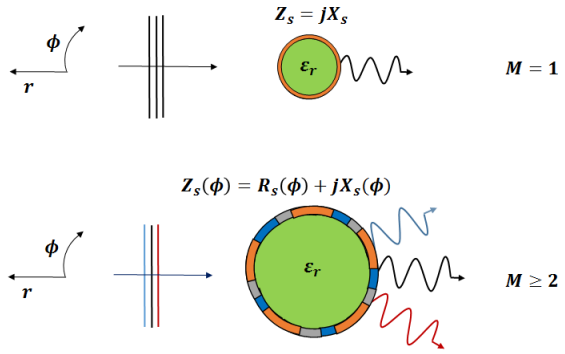

Figure 1. Subwavelength dielectric particle with a mantle cloak Z_s, which is demonstrated to be purely imaginary for the suppression of a single dominant harmonic wave ($M = 1$, top). Dielectric particle beyond quasi-static condition, with attached mantle cloak Z_s, which is demonstrated to be of complex value with oscillating azimuthal values for the suppression of multiple dominant harmonic waves ($M \geq 2$, bottom).

use of an impedance metasurface [21] wrapped as a mantle cloak, it is demonstrated how zero external scattering is a sufficient condition to generate parity-time radiationless sources.

2. Generalization on multi-harmonic mantle cloaking for dielectric obstacles

Let us consider a non-magnetic dielectric cylinder of radius a, with axis aligned to $\hat{z}$, having relative permittivity ε_r, directly loaded by an impedance sheet at its boundary $r = a$. According to Mie Theory, the overall scattering problem is developed for normal incidence, under the assumption of Transverse Magnetic (TM_z) illumination with respect to the z-axis of the dielectric cylinders [22]. In cartesian coordinates, this means possessing wavenumber $\vec{k} = k_x\hat{x}$, electric field $\vec{E} = E_z\hat{z}$ and magnetic field $\vec{H} = -H_y\hat{y}$. In the cylindrical coordinate system (r, ϕ, z), the total tangential electromagnetic fields are given by [22]

$$\mathrm{E}_z(r,\phi) = \begin{cases} \displaystyle\sum_{m=-\infty}^{m=+\infty} j^m \mathrm{e}_m(kr)\mathrm{e}^{-jm\phi} & , \quad r \le a \\ \displaystyle\sum_{m=-\infty}^{m=+\infty} j^m \mathrm{g}_m(k_b r)\mathrm{e}^{-jm\phi} & , \quad r \le a \end{cases} \tag{1}$$

$$\mathrm{H}_\phi(r,\phi) = \begin{cases} \dfrac{-j}{\omega\mu_b} \displaystyle\sum_{m=-\infty}^{m=+\infty} j^m \mathrm{e}'_m(kr)\mathrm{e}^{-jm\phi} & , \quad r \le a \\ \dfrac{-j}{\omega\mu_b} \displaystyle\sum_{m=-\infty}^{m=+\infty} j^m \mathrm{g}'_m(k_b r)\mathrm{e}^{-jm\phi} & , \quad r \ge a \end{cases} \tag{2}$$

where $k_b = \omega\sqrt{\varepsilon_b\mu_b}$ and $k = \sqrt{\varepsilon_r}k_b$ are the wavenumbers in the background region (with absolute permittivity ε_b and permeability μ_b) and in the dielectric cylinder (with relative permittivity ε_r), respectively. The magnetic field can be directly derived from Maxwell's equations as $H = j\nabla \times E/\omega\mu_b$. Throughtout the paper, the time convention $e^{+j\omega t}$ is tacitly assumed. The unknown radial functions $e_m(\cdot)$ and $g_m(\cdot)$ contain the expansion coefficients related to the cylindrical harmonics as

$$\mathrm{e}_m(kr) = a_m J_m(kr) \tag{3}$$

$$\mathrm{g}_m(k_b r) = J_m(k_b r) + c_m H_m^{(2)}(k_b r) \tag{4}$$

where $J_m(\cdot)$ is the Bessel function of m-th order, whereas $H_m^{(1)}(\cdot)$ - and $H_m^{(2)}(\cdot)$ - are the m-th order first (and second) Hankel functions. This analytical model can be profitably adopted not only for the suppression of incoming plane waves, but also for the case of incident Bessel (or arbitrary shaped) beams [23, 24]. The coefficient a_m is related to the internal total field (of interest for nonradiating problems), whereas the coefficient c_m is related to the external scattered field (of interest for cloaking problems). The tangential fields at the interface $r = a$ are imposed as

$$\mathrm{E}_z(a^-,\phi) = \mathrm{E}_z(a^+,\phi) \tag{5}$$

$$Y_s\ \mathrm{E}_z(a^-,\phi) = \mathrm{H}_\phi(a^+,\phi) - \mathrm{H}_\phi(a^-,\phi) \tag{6}$$

where 5 ensures the continuity of the tangential electric field, whereas, 6 for the magnetic field can be rewritten as

$$Y_s(\phi) = \left[\frac{\mathrm{H}_\phi(a^+,\phi)}{\mathrm{E}_z(a^+,\phi)} - \frac{\mathrm{H}_\phi(a^-,\phi)}{\mathrm{E}_z(a^-,\phi)}\right] = Y_b(\phi) - Y_u(\phi) \tag{7}$$

where Y_s is the surface admittance attached to the external surface at $r = a^+$. From these boundary conditions, the unknown expansion coefficients a_m and c_m (implictly related to the TM_z scattering) can be automatically obtained. The TE_z scattering case, for which $\vec{E} = E_y\hat{y}$ and $\vec{H} = H_z\hat{z}$, can be derived by duality as suggested for metallic objects in [20].

As observed for single harmonic wave cancellation in [19], the surface admittance $Y_s(\cdot)$ is computed as the residual difference between two other functions: the background admittance $Y_b(\cdot)$ in the outer region at $r = a^+$ and the unloaded admittance $Y_u(\cdot)$ seen from the region at $r = a^-$. It is worthwhile mentioning that they are all explicit functions of the azimuthal angle ϕ. When the cloaking condition $c_m = 0$ is imposed (ideally for any harmonic wave index m) and the internal fields within the dielectric cylinder are obtained accordingly, 7 can be interpreted as a cylindrical matching mechanism [19] in order to ensure to zero the discontinuity between the background admittance Y_b and the sum of unloaded and surface admittances $Y_u + Y_s$. In the following, the admittance values will be considered as normalized with respect to the intrinsic admittance of the background $Y_B = k_b/\omega\mu_b$.

In this work, multiple dominant cylindrical waves may contribute simultaneously to the higher-order scattering, hence a multi-harmonic mantle cloaking design is here addressed. This approach generalizes the works on single harmonic cancellation for dielectric particles in [19] and conductive obstacles in [20]. From the definition of background admittance as the ratio of external tangential magnetic and electric fields, in the cylindrical reference system the normalized background admittance $\tilde{Y}_b(\phi)$ becomes

$$\widetilde{Y}_b(\phi) \equiv \frac{Y_b(\phi)}{Y_B} = -j\frac{\displaystyle\sum_{m=-\infty}^{m=+\infty} j^m J'_m(k_b a)\mathrm{e}^{-jm\phi}}{\displaystyle\sum_{m=-\infty}^{m=+\infty} j^m\ J_m(k_b a)\ e^{-jm\phi}} \tag{8}$$

computed, by definition, as the ratio of external magnetic and electric fields. In fact, in the background scenario, the solution for the continuity of tangential electromagnetic fields by a bare particle with $\varepsilon = 1$

is trivial: it gives $a_m = 1$ and $c_m = 0$ for all the m-harmonics and at all frequencies (k_b), thus no scattered fields are excited due to the continuity in the permittivity values.

It appears to be non-trivial to investigate with the same methodology, if a bare dielectric particle, with a relative permittivity greater than one (as for natural dielectrics) can still have no outgoing scattered fields ($c_m = 0$) when it is excited, understanding under which conditions this phenomenon takes place. By imposing the boundary conditions for the continuity of tangential electric and magnetic fields, the radiationless condition $c_m = 0$ for all m-harmonics can be imposed, so that

$$a_m J_m(ka) = J_m(k_b a) \tag{9}$$

$$a_m \sqrt{\varepsilon_r} J'_m(ka) = J'_m(k_b a) \tag{10}$$

Such results are valid in a narrow frequency bandwidth, in which

$$\frac{J'_m(k_b a)}{J_m(k_b a)} - \frac{\sqrt{\varepsilon_r} J'_m(ka)}{J_m(ka)} = 0 \tag{11}$$

that is a function of the cylinder radius a, and of the particle relative permittivity ε_r. As highlighted in [19] for the single-harmonic cancellation case, it is convenient to control the generation of such a radiationless phenomenon in a bare particle, by inserting an additional term in 11. Since all these terms are dimensionally admittances (since they appear as the imaginary part of the ratio between magnetic and electric fields), a proper surface admittance load Y_s can be inserted to control the phenomenon, in order to achieve zero external scattered field condition. The numerator in the second term of 11 can be interpreted as the internal magnetic field $H_\phi(a^-, \phi)$ in the dielectric region derived in 7, thus it can be associated to the normalized unloaded admittance $\widetilde{Y}_u(\phi)$, with the same methodology, computed as

$$\widetilde{Y}_u(\phi) \equiv \frac{Y_u(\phi)}{Y_B} = -j \frac{\sum_{m=-\infty}^{m=+\infty} j^m \sqrt{\varepsilon_r} J'_m(ka) \mathrm{e}^{-jm\phi}}{\sum_{m=-\infty}^{m=+\infty} j^m J_m(ka) \mathrm{e}^{-jm\phi}} \tag{12}$$

It is worthwhile mentioning that the unloaded admittance computed here has not to be confused with the one of a purely bare dielectric cylinder, but it has been assumed that no external scattered fields can bee excited. For this reason, it is possible to exploit 12 in 7, in order to control the final design formula for multi-harmonic admittance mantle cloak as

$$\widetilde{Y}_s(M, \phi) \approx -j \frac{\sum_{m=-M}^{m=+M} j^m \ \Delta_m J_m(k_b a) \ e^{-jm\phi}}{\sum_{m=-M}^{m=+M} j^m J_m(k_b a) \mathrm{e}^{-jm\phi}} \tag{13}$$

where

$$\Delta_m = \frac{J'_m(k_b a)}{J_m(k_b a)} - \sqrt{\varepsilon_r} \frac{J'_m(ka)}{J_m(ka)} \tag{14}$$

it is the non-zero residual difference needed to compensate the admittance variation between background and dielectric contributions. As expected, if $\varepsilon_r \approx 1$, then $k \approx k_b$ and 11 is automatically zero: no cloak is needed. In addition, if 11 is already satisfied for certain frequencies, $\Delta_m = 0$ and no surface admittance is needed, since the bare dielectric particle is already behaving at its surface boundary like an infinite impedance load.

The formula in 13 is derived without any approximation and under any frequency regime (quasi-static and beyond), once it has been ensured that all the dominant harmonic waves M are taken into account in the summation. The surface admittance function appears to be highly dependent from $\Delta_m(\cdot)$, which represents the residual correction term needed to make the external total field equal to the incident one (no external scattered fields). It is worthwhile mentioning that now the series has been truncated to a finite value M, which represents the number of harmonic waves that is possible to suppress with such a thin impedance cloak design: in the ideal case of zero scattered fields for all the cylindrical harmonics, $M \to \infty$. In the simplified case of single harmonic suppression, 13 reduces to $\widetilde{Y}_s(m = n) = -j\Delta_n(k_b a, \varepsilon_r)$, which is consistent with the design equation found in [19], where the scattering suppression of a single single dominant harmonic wave has been pursued (the choice of the single harmonic index $m = n$ to cancel is due to the highest level of undesired external scattered energy). In quasi-static regime, the choice is not arbitrary since the major scattering contribution is related to the lowest harmonic wave ($m = 0$ in 2D objects), but in other frequency regimes it could be sufficient to detect the higher-order dominant wave to suppress ($m = n$, with n as an arbitrary integer number, for example $m = 1$ or $m = 3$). To notice that, for single dominant wave suppression, the surface admittance function does not anymore depend on the azimuthal coordinate ϕ due to its simplification in the exponential terms. In such a multi-harmonic case, an oscillating azimuthal dependence starts appearing with specific real and imaginary admittance/impedance values as it is evident from 13, thus a general trade-off holds between the complexity of the mantle cloak and the chosen set of harmonic waves M. For simultaneous scattering cancellation, the more the harmonic terms to suppress, the more the harmonic terms present in the surface impedance function, which turns out to be of complex value due to the simultaneous cancellation of several higher-order harmonic modes. Moreover,

as it can be deduced from 13, the surface admittance function satisfies the parity-time condition, since it is a general property of symmetric and lossless devices. As also reported in the specific case of cloaking a metallic cylinder [16], a balanced loss and gain condition holds for the admittance functions, giving rise to an oscillating behaviour of the real part (with zero mean value) and imaginary part along the azimuthal direction.

3. Numerical results for Scattering Cross Section and Electromagnetic Fields localization

In this work, we investigate the ability to control more than one harmonic wave in contrast with the previous cases of single-harmonic wave suppression [19, 20]. To this purpose, the scattering suppression can be estimated with respect to uncloaked case, by defining a scattering cross section (SCS) gain G_{SCS} as

$$G_{SCS}(f) = \frac{\sum_{-M}^{+M} |c_m(f)|^2_{clk}}{\sum_{-M}^{+M} |c_m(f)|^2_{unc}} \tag{15}$$

where *unc* and *clk* stand for uncloaked and cloaked cases, respectively. In Fig. 2, it is reported the SCS gain as first introduced in [19], in order to evaluate the scattering suppression (negative sign) or scattering enhancement (positive sign) in a finite frequency bandwidth (in terms of normalized size a/λ) with respect to the bare dielectric case, after the insertion of the impedance coating.

Even if all the 2D harmonics M contribute to the scattering with different weights, there exists a number of independent cylindrical harmonics M_{max} which are sufficient to accurately compute G_{SCS}, since with M_{max} cylindrical modes it is possible to accurately represent the entire scattered fields. According to electromagnetic inverse scattering strategies [25], for a 2D geometry possessing circular symmetry, these independent basis functions are the cylindrical harmonic waves and the value is

$$M_{max} = 2k_b a \tag{16}$$

according to [25], where it can be noticed that the only variable involved in the determination of M_{max} is not the relative permittivity of the bare object ε_r, but its radius a normalized to the wavelength of the incoming field (even if the permittivity plays a role in the amount of scattered energy that is reflected or transmitted from one point to another).

In Fig. 2, the scattering suppression for a dielectric object with $a = 0.3\lambda$ is considered, highlighting its narrowband frequency behaviour [16]. For this case, $M_{max} \approx 4$ and this is the number of independent harmonic waves to suppress in order to achieve a deep SCS gain: since M_{max} does not depend

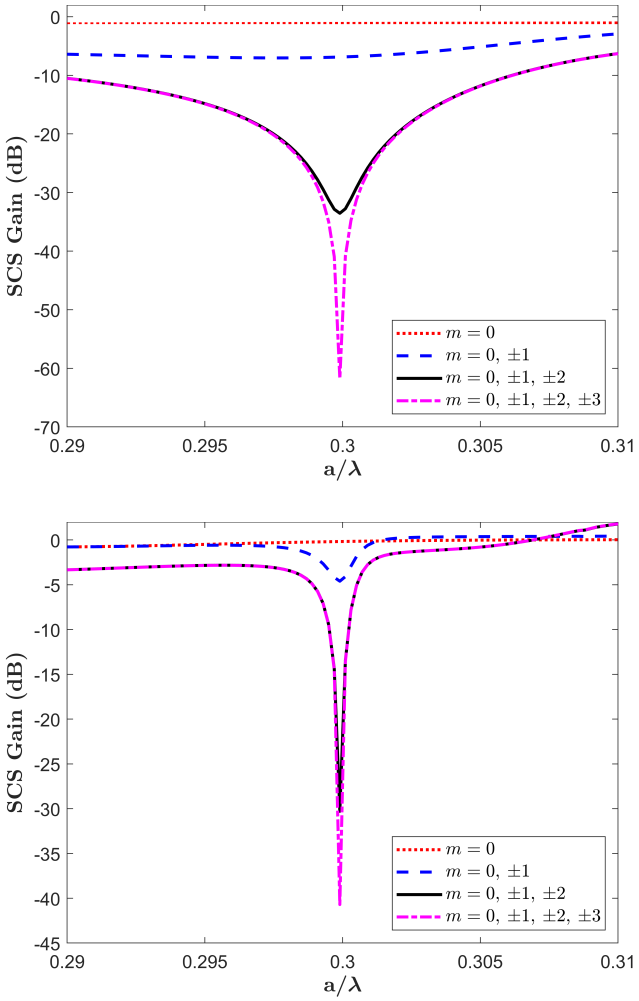

Figure 2. SCS Gain for a bare dielectric particle with $a/\lambda = 0.3$ possessing $\varepsilon_r = 3$ (top) or with $\varepsilon_r = 15$ (bottom) as a function of the m-harmonics that have been suppressed.

on the permittivity value, this is demonstrated to be valid for a dielectric object with $\varepsilon_r = 3$ in Fig. 2 (top) and for a dielectric object with $\varepsilon_r = 15$ in Fig. 2 (bottom). The choice of low or high values for the dielectric permittivity is arbitrary, since this theory can be applied to both cases since no approximation is included in the scattering model. In addition, metallic loading is not present in the scattering problem and the cloaking mechanism is directly modeled via a thin surface impedance layer: more details about the dispersion modeling with metallic objects and loads can be found in [20],[16]. As expected, the more the number of cylindrical harmonic waves to be suppressed, the deepest are the SCS gain values whereas, at the same time, the frequency bandwidth becomes narrower and narrower. It is worthwhile noticing that in Fig. 2 (bottom), the SCS Gain is even higher than the uncloaked case at higher frequencies.

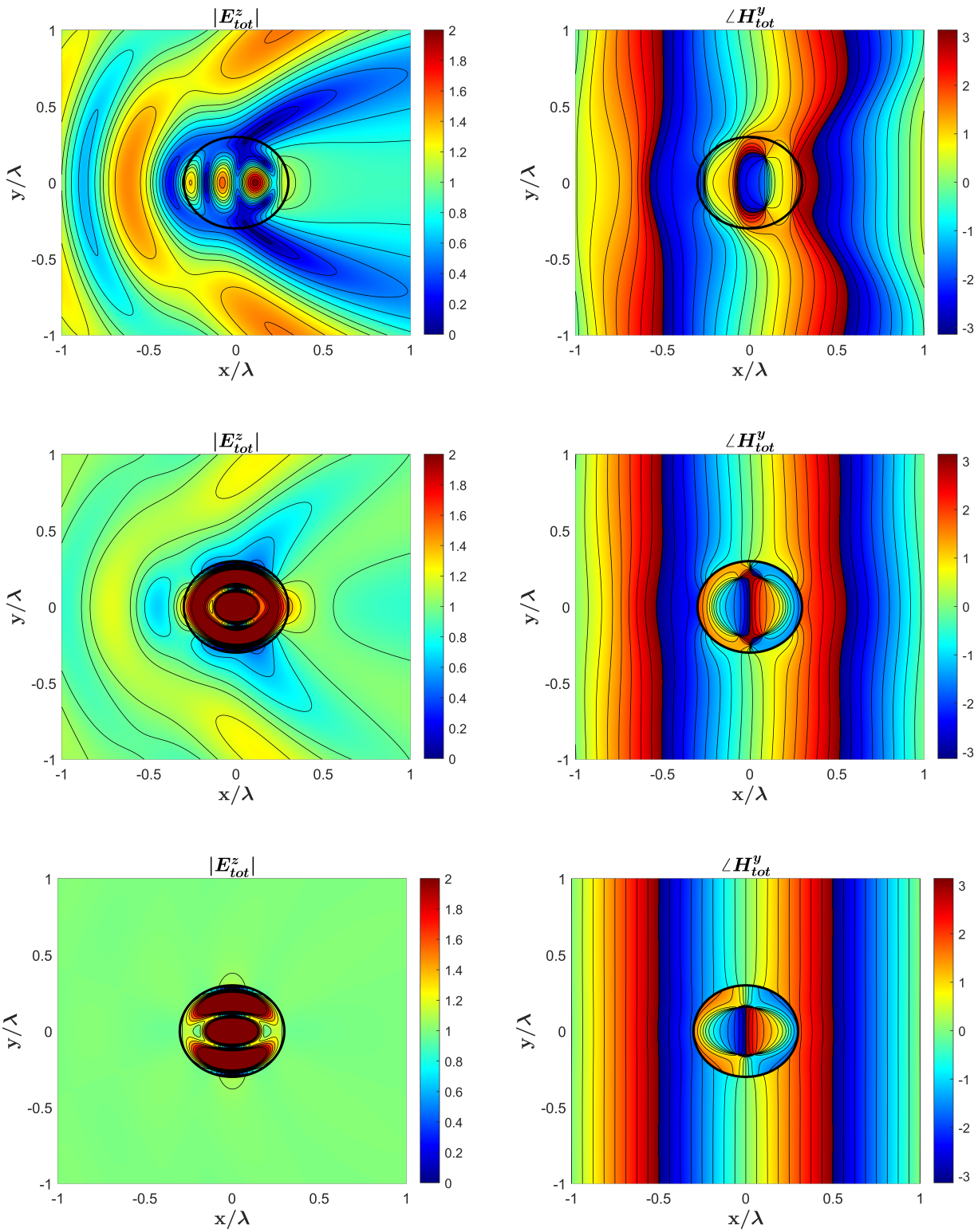

Figure 3. [same scale, interest for external fields] Magnitude of the total electric (left) and phase of the total magnetic (right) fields for a dielectric object with radius $a = 0.3\lambda_b$ and relative permittivity $\varepsilon_r = 9$ (bare case, top) and with the insertion of the multi-harmonic mantle cloak with $M = 2$ and $M = 4$ (bottom).

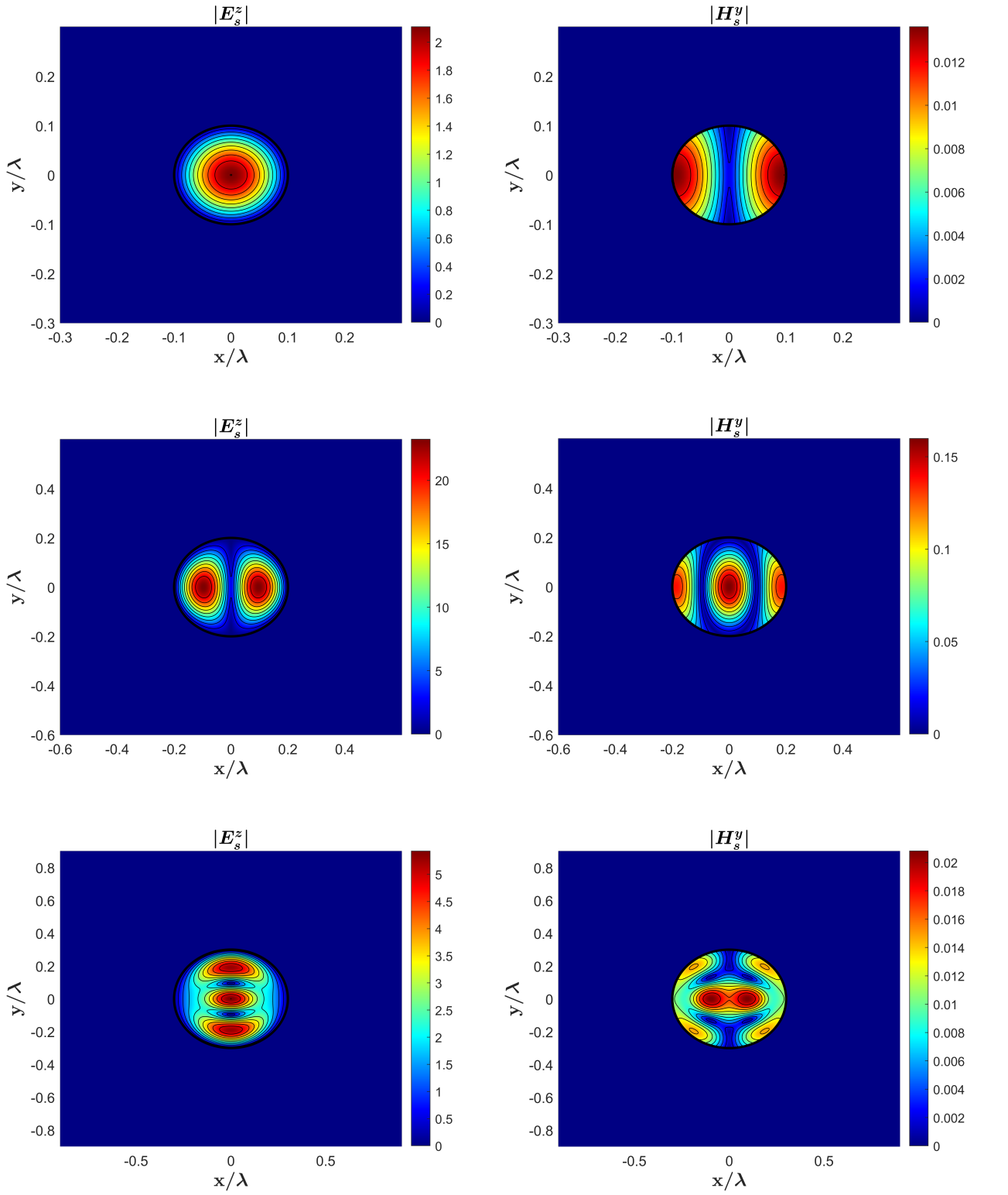

Figure 4. [different scale, interest for internal fields] Magnitude of the scattered electric (left) and magnetic (right) fields for a dielectric object with relative permittivity $\varepsilon_r = 9$ and with radius $a = 0.1\lambda_b$ (1st row), $a = 0.2\lambda_b$ (2nd row), $a = 0.3\lambda_b$ (3rd row).

This is consistent with the fact that the integral of the energy spectrum, while cloaking lossless objects, has been demonstrated to be a constant: if it dramatically decreases in the designed bandwidth, it has to increase in other frequency regions (the cloaked object scatters more in [26]).Interestingly, this is consistent with the frequency analysis performed on nonradiating anapole modes [4, 5, 6, 27]. In order to get an insight on the nonradiating phenomenon, let us consider the behaviour of the electromagnetic fields generated by the scattering of a bare dielectric cylinder, with a relative permittivity between these two cases ($\varepsilon_r = 9$) and overall diameter $a = 0.3\lambda_b$ (free-space is assumed as background material, thus $\lambda_b = \lambda_0$). The mantle cloak is directly attached to the object surface and, by exploiting 13, a proper complex surface impedance function $Z_s(\phi)$ is determined for a given set of M harmonic components.

From the plots of Fig. 3, where the magnitude of the total electric field component E_z and phase of the total magnetic field component H_y are reported, the evolution of the multi-harmonic cancellation can be appreciated with respect to the bare case (top): in this reference system, the impinging incident direction is from $+\hat{x}$. Since the multiple scattered waves generated by the obstacle are reducing their amplitude in the external region of the dielectric object (lossless, for simplicity), the cancellation mechanism is actually hiding the electromagnetic energy inside its internal domain, as it can be appreciated by considering the *same* color scale values for the different plots of the *external* total electric field magnitude $|E_z|$ with reference to the uncloaked case (top).

For the case of $a = 0.3\lambda$, $M_{max} = 3.77 \approx 4$ and the M-harmonic wave cancellation is reported by considering $M = 2$ and $M = 4$, highlighting the improved evolution in suppressing the scattered energy. In Fig. 3, as the two cylindrical waves with $m = 0, 1$ are suppressed ($M = 2$), the total electric field starts decreasing behind the object, while mitigating the reflected energy in front of the dielectric obstacle. The further suppression of $M = 4$ harmonic waves keeps the total electric field around the incident wave value of 1 V/m (green region). The internal electric field within the dielectric cylinder behaves as a radiationless source, since the electromagnetic field is trapped inside as a cylindrical cavity mode and the total magnetic field phase front becomes similar to a plane wave in the external domain. This analysis is valid for a fixed incident direction, because in 13 there is a dependence on the electric field configuration: this effect reduces to consider the phenomenon as unidirectional cloaking, as highlighted in [16]. Once suppressed all the dominant M_{max} harmonic waves, this work does not focus on the unidirectionality issue, but on the internal electromagnetic field configurations as a function of the scatterer dimension normalized to the incoming wavelength.

For the same case of scattering by a dielectric obstacle with $\varepsilon_r = 9$, in Fig. 4 the magnitude of the scattered electric (left) and magnetic (right) fields is reported for various radii in terms of impinging wavelength (M_{max} is fixed to the maximum radius normalized to the incoming wavelength, in order to obtain always a nonradiating source). In Fig. 4 (1st row), it is reported the case when $a = 0.1\lambda_b$ and the dominant harmonic wave which is suppressed is the one with $m = 0$, since the dielectric particle is in subwavelength conditions. In Fig. 4 (1st row, left), the electric field configuration assumes the characteristic pattern of an elementary point source (this is expected due to quasi-static conditions [19]), with concentric cylindrical waves, that are nonradiating since at the same time the magnetic field is oscillating as reported in Fig. 4 (1st row, right), with high field value around its cylindrical boundary. As the size of the dielectric particle (in terms of wavelength) increases, the configuration of the electric field starts complicating as a collection of elementary nonradiating sources, with high field values (notice the different color scale values) in the internal region of the dielectric. At the same time, in Fig. 4 (2nd row, right), the magnetic field is oscillating with high field value at the center (where the electric field is minimum) and also around its cylindrical boundary. In Fig. 4 (3rd row), it is reported the scattered field for the case as analyzed in terms of total fields in Fig. 3 (lst row), with electric and magnetic field radiation patterns that are automatically generated in order to be a nonradiating source.

4. Conclusions

A generalization of a multi-harmonic surface impedance cloak has been proposed in this work, with respect to dominant single-harmonic wave cancellation. A theoretical model based on equivalent admittances has been proven to hold also for the case of multi-harmonic cancellation. Moreover, it has been revealed that, beyond the quasi-static regime or single-dominant harmonic wave approximation, the surface impedance layer covering a dielectric object has to be shaped with a variable azimuthal profile. Numerical results have confirmed that low and high permittivity particles show the same maximum number of harmonic waves M_{max} to be considered for the electromagnetic field representations. Such harmonics can be fully represented and simultaneously suppressed. The potential of a multi-harmonic impedance mantle boundary condition can be useful not only for controlling the cloaking

effect, but also for modeling higher-order radiationless sources. Possible implementations of a proper impedance boundary can be performed by surrounding a dielectric object with all-dielectric clusters [28] or, with the same formalism, a metallic cylinder with a local azimuthally varying impedance metasurface as thin patterned sinusoidally-shaped loads [29] or with balanced loss and gain [16].

References

[1] A. J. Devaney and E.Wolf, "Radiating and nonradiating classical current distributions and the fields they generate", Phys. Rev. D 8, 1044 (1973).

[2] E. Hurwitz and G. Gbur, "Null-field radiationless sources", Opt. Lett., Vol. 39, No. 22 (2014).

[3] F. Monticone and A. Alù, "Embedded Photonic Eigenvalues in 3D Nanostructures", Phys. Rev. Lett. 112 (213903), 2014.

[4] A. E. Miroshnichenko, A. B. Evlyukhin, Y. F. Yu, R. M. Bakker, A. Chipouline, A. I. Kuznetsov, B. Luk'yanchuk, B. N. Chichkov and Y. S. Kivshar, "Nonradiating anapole modes in dielectric nanoparticles", Nat. Commun. 6, 8069 (2015).

[5] W. Liu, J. Zhang, B. Lei, H. Hu, A. E. Miroshnichenko, "Invisible nanowires with interfering electric and toroidal dipoles", Opt. Lett., Vol. 40, No. 10 (2015)

[6] N. A. Nemkov, A. A., Basharin, V. A. Fedotov, "Nonradiating sources, dynamic anapole, and Aharonov-Bohm effect", Phys. Rev. B 95, 165134 (2017).

[7] K. V. Baryshnikova, D. A. Smirnova, B. S. Luk'yanchuk and Y. S. Kivshar, "Optical Anapoles: Concepts and Applications", Advanced Optical Materials (2019).

[8] A. Alù, N. Engheta, "Achieving transparency with plasmonic and metamaterial coatings", *Phys. Rev. E*, Vol. 72, Issue 1, Article 16623, 9 pp. (2005).

[9] A. Monti, F. Bilotti, A. Toscano, "Optical cloaking of cylindrical objects by using covers made of core–shell nanoparticles", *Opt. Lett.* 36, pp. 4479-4481 (2011)

[10] E. Shokati, N. Granpayeh, and M. Danaeifar, "Wideband and multi-frequency infrared cloaking of spherical objects by using the graphene-based metasurface", Appl. Opt. 56, pp. 3053-3058 (2017).

[11] E. Bor, C. Babayigit, H. Kurt, K. Staliunas, and M. Turduev, "Directional invisibility by genetic optimization", *Opt. Lett.* 43, 5781-5784 (2018).

[12] U. Leonhardt, T. G. Philbin, *Geometry and Light: The Science of Invisibility* (Dover, Mineola, 2010).

[13] E. Martini, S. Maci, and A. D. Yaghjian, Cloaking in terms of nonradiating cancelling currents, Chap. 11 in Selected Topics in Photonic Crystals and Metamaterials, edited by A. Andreone, A. Cusano, A. Cutolo, and V. Galdi (World Scientific, Singapore), 2011.

[14] A. Alù, "Mantle cloak: Invisibility induced by a surface", *Phys. Rev. B*, Vol. 80, 245115, 2009.

[15] P. -Y. Chen, A. Alù, "Mantle cloaking using thin patterned metasurfaces", *Phys. Rev. B*, Vol. 84, 205110, 2011.

[16] D. Sounas, R. Fleury, A. Alù, "Unidirectional Cloaking Based on Metasurfaces with Balanced Loss and Gain", Phys. Rev. Applied 4 (0140059), 2015.

[17] G. Labate, L. Matekovits, "Invisibility and cloaking structures as weak or strong solutions of Devaney-Wolf theorem", *Optics Express*, Vol. 24, No. 17, pp. 19245-19253, 2016.

[18] G. Labate, A. K. Ospanova, N. A. Nemkov, A. A. Basharin, L. Matekovits, "Nonradiating Anapole Condition Derived from Devaney-Wolf Theorem and Excited in a Broken-Symmetry Dielectric Particle", *Optics Express*, 2020 (to appear, available at: arxiv.org/abs/1806.04134).

[19] G. Labate, A. Alù, L. Matekovits, "Surface-admittance equivalence principle for nonradiating and cloaking problems", Phys. Rev. A, 95 (063841) 2017.

[20] G. Labate, S. K. Podilchak, L. Matekovits, "Closed-form harmonic contrast control with surface impedance coatings for conductive objects", Vol. 56, No. 36, Applied Optics (2017).

[21] Oscar Quevedo-Teruel et al., "Roadmap on Metasurfaces", J. Opt. 21 (073002), 2019.

[22] C. A. Balanis, *Advanced engineering electromagnetics*, Ch. 11, (Wiley, New York, 1989).

[23] S. C. Pavone, A. Mazzinghi, A. Freni and M. Albani, "Comparison between broadband Bessel beam launchers based on either Bessel or Hankel aperture distribution for millimeter wave short pulse generation", *Optics Express*, Vol. 25, No. 16 (2017).

[24] D. Comite, W. Fuscaldo, S. C. Pavone, G. Valerio, M. Ettorre, M. Albani, A. Galli, "Propagation of nondiffracting pulses carrying orbital angular momentum at microwave frequencies", Appl. Phys. Lett. 110 (11), 114102, 2017.

[25] O. M. Bucci and T. Isernia, "Electromagnetic inverse scattering: Retrievable information and measurement strategies", *Radio Science*, Vol. 32, No. 6, Pages 2123-2137, 1997.

[26] F. Monticone, A. Alù, "Do Cloaked Objects Really Scatter Less?", Physical Review X 3, 041005 (2013).

[27] B. Luk'yanchuk, R. Paniagua-Domínguez, A. I. Kuznetsov, A. E. Miroshnichenko and Y. S. Kivshar, "Hybrid anapole modes of high-index dielectric nanoparticles", Phys. Rev. A., 95, 063820 (2017)

[28] A. K. Ospanova, G. Labate, L. Matekovits, and A. A. Basharin, "Multipolar passive cloaking by nonradiating anapole excitation", Sci. Rep., vol. 8, no. 1, p. 12514 (2018).

[29] L. Matekovits, T. Bird, "Width-modulated Microstripline based Mantle Cloaks for Thin Single-and Multiple Cylinders", IEEE Trans. on Antennas and Prop.,Vol. 62, No. 5, 2014.